Electronic Supplementary Material (ESI) for RSC Advances

Cite this: DOI: 10.1039/c0xx00000x

www.rsc.org/xxxxxx

ARTICLE TYPE

Supplementary information Water-Mediated Structural Tunability of Alkyl/siloxane Hybrid: from Amorphous to Lamellar Structure or Bilamellar Superstructure

S. C. Nunes[a,b,c], N. J. O. Silva[d], J. Hümmer[a], R. A. S. Ferreira[d], P. Almeida[c,e], L. D. Carlos[d], V. de Zea Bermudez[a,b]*

Scheme S1. Synthetic procedure of the m-A(x) and AC-m-A(8) (1:y) mono-amidosils. PC is palmitoyl chloride e DC is decanoyl chloride

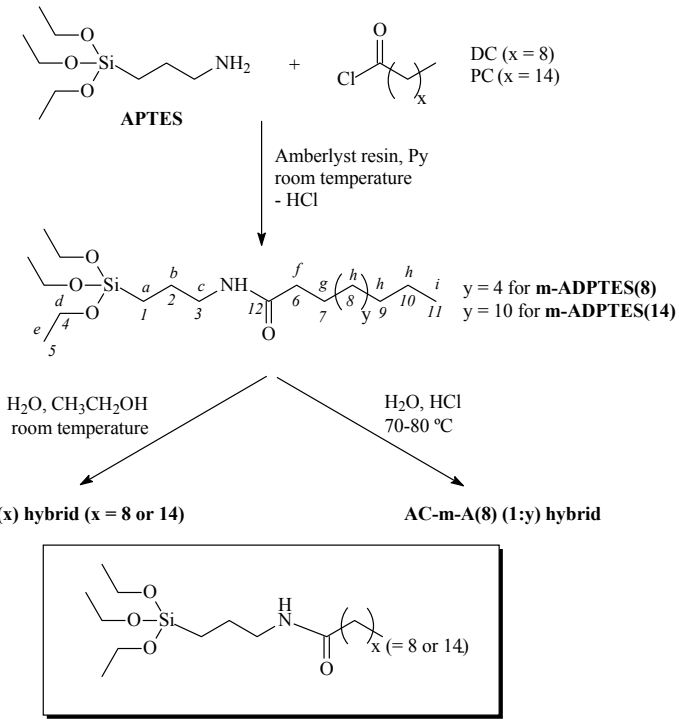

Cite this: DOI: 10.1039/c0xx00000x

www.rsc.org/xxxxxx

Table S1. Relevant details of the synthesis of the m-A(x) and AC-mA(8) (1:y) mono-amidosils

	m-ADPTES(x) mono-amidosil precursors	
Materials	**x = 14**[1]	**x = 8**
DC/PC	1.000 mL (3.30 mmol)	1.000 mL (4.80 mmol)
APTES	0.774 mL (3.30 mmol)	1.132 mL (4.80 mmol)
Amberlyst resin	0.841 g (3.90 mmol)	1.333 g (6.20 mmol)
Py	53 µL (0.66 mmol)	77 µL (0.90 mmol)
THF	30 mL	40 mL

	m-A(x) mono-amidosils *via* the classical route *via* the classical route		**m-A(8) (1:y) mono-amidosil *via* the acid-catalized hydrolytic route**		
Materials	**x = 14**[1]	**x = 8**	**y = 600**	**y = 300**	**y = 100**
CH_3CH_2OH	769 µL (13.2 mmol)	1.124 mL (19.3 mmol)	-	-	-
H_2O	118 µL (6.60 mmol)	173 µL (9.63 mmol) 10 mL	-	-	-
THF	10 mL	-	-	-	-
H_2O	-	-	51.8 mL (2880 mmol)	25.9 mL (1440 mmol)	8.6 mL (480 mmol)
HCl (1M)	-	-	960 µL (0.96 mmol)	960 µL (0.96 mmol)	480 µL (0.48 mmol)

Cite this: DOI: 10.1039/c0xx00000x

www.rsc.org/xxxxxx

ARTICLE TYPE

Table S2. ^{1}H [$CDCl_3$; δ (ppm), *J*(Hz)] and ^{13}C [$CDCl_3$; δ (ppm)] NMR and FT-IR data of the m-ADPTES(8) precursor.

NMR						
^{1}H ($CDCl_3$)					^{13}C ($CDCl_3$)	
δ (ppm)		*J* (Hz)		Attribution	δ (ppm)	Attribution
4.02	6H	q	6.9	H^d	176.4	C^{12}
3.55	2H	q	6.8	H^c	57.71	C^4
2.15	2H	t	7.0	H^f	41.78	C^3
1.66-1.59	4H	m	-	H^b, H^g	36.42	C^6
1.257-1.201	21H	m	-	H^e and H^h	31.64	C^9
0.899-0.849	3H	t	6.4	H^i	29.28-28.9	C^8 (4C)
0.60	2H	m	-	H^a	25.37	C^7
					24.77	C^2
					22.43	C^{10}
					18.05	C^5
					13.99	C^{11}
					13.83	C^1

FT-IR	
$\overline{V}$ (cm^{-1})	Attribution
3293	νNH
3082	νNH
2955	$\nu_{as}CH_3$
2925	$\nu_{s}CH_2$
1737	νC=O
1644	νC=O
1551	δNH

Cite this: DOI: 10.1039/c0xx00000x

www.rsc.org/xxxxxx

Table S3. .^{13}C CP/MAS and ^{29}Si MAS NMR data of the m-A(x) and AC-m-(8) (1:600) mono-amidosils.

^{13}C CP/MAS				^{29}Si MAS			
δ (ppm)				δ (ppm) (A[a])			
m-A(x)		AC-m-A(8)	Attribution	m-A(x)		AC-m-A(8) (1:600)	Attribution
x = 8	x = 14[1]Error!	(1:600)		x = 8	x = 14[1]		
174	174	173	C^{12}	-53.8 (13.7)	-49.5 (8.5)	-53.1 (3.4)	T^1
42	42	43	C^3	-58.9 (33.4)	-57.8 (59.9)	-57.7 (50.2)	T^2
36	36	37	C^6	-66.9 (52.9)	-67.0 (31.6)	-66.1 (46.4)	T^3
32	34	34	C^9	83	74	73	c[b]
-	32	33	C^8 *trans*	$R´Si(OH)_{0.6}(O)_{1.2}$	$R´Si(OH)_{1.1}(O)_{0.8}$	$R´Si(OH)_{1.2}(O)_{0.7}$	Empirical Formula
30	-	30	C^8 *gauche*				
26	26	27	C^7				
23	24	24	C^2/C^{10}				
-	-	23	C^{10}				
14	14	14	C^{11}				
11	11	12	C^1				

[a] Integrated area in % ; [b]c (polycondensation degree) = $1/3(\%T^1 + 2\%T^2 + 3\%T^3)\times100$; [c] $R'=CH_3(CH_2)_xC(=O)NH\text{-}(CH_2)_3$

Cite this: DOI: 10.1039/c0xx00000x

www.rsc.org/xxxxxx

Table S4. Characteristic bands of FT-IR and FT-Raman of the m-A(x) and AC-m-A(8) (1:600) mono-amidosils in the ν_aCH_2, ν_sCH_2, δCH_2, amide I, amide II modes and νC-C region. Wavenumbers in cm^{-1}.

m-A(x)				AC-m-A(8) (1:600)		Atribuition	
x = 8		x = 14					
FT-IR (fwhm) (A^a) (I^b)	FT-Raman	FT-IR (fwhm) (A) (I^b)	FT-Raman	FT-IR (fwhm) (A) (I^b)	FT-Raman		
	2929	-	2925	-	2925	Fermi Ressonance of ν_sCH_2 fundamental with δCH_2 overtones	
2929 (34) (45) (0.28)	-	-	-	-		ν_aCH_2	*gauche* conformations
-	-	2919 (21) (52) (2.2)	-	2924 (29) (49) (0.95)	-		all-*trans* conformations
-	2890	-	-	-	-		*gauche* conformations
-	-	-	2880	-	2881		all-*trans* conformations
-	2851	-	2858	-	2860	ν_sCH_2	*gauche* conformations
2856 (10) (11) (0.16)	-	-	-	-	-		*gauche* conformations
-	-	2850 (10) (19) (1.5)	-	2852 (14) (13) (0.50)	-		all-*trans* conformations
-	-	-	2845	-	2846		all-*trans* conformations
1676 (34) (12) (0.073)	-	-	-	-	-	amide I	"free" C=O groups
1657 (24) (19) (0.13)	-	1652 (27) (24) (0.46)	-	1656 (28) (18) (0.38)	-		disordered aggregates
1643 (20) (17) (0.23)	-	1640 (17) (33)(0.96)	-	1640 (20) (22) 0.62)			ordered aggregates
1626 (20) (10) (0.11)	-	1625 (15) (5) (0.17)	-	1622 (29) (20) (0.40)	-		ordered aggregates
1560 (38) (25) (0.12)	-	1560 (24) (23) (0.48)	-	1558 (35) (21) (0.34)	-	amide II	
1540 (31) (16) (0.14)	-	1545 (25) (15) (0.32)	-	1542 (34) (19) (0.33)	-		
-	-	-	-	-	1127		all-*trans* conformations
-	1121		-		-		*gauche* conformations
-	1078		-		-	νC-C	*gauche* conformations
-	1064		-				*gauche* conformations
-		-	1062	-	1062		all-*trans* conformations

Integrated area in %, b – intensity ; fwhm - full width at half maximum

Cite this: DOI: 10.1039/c0xx00000x

www.rsc.org/xxxxxx

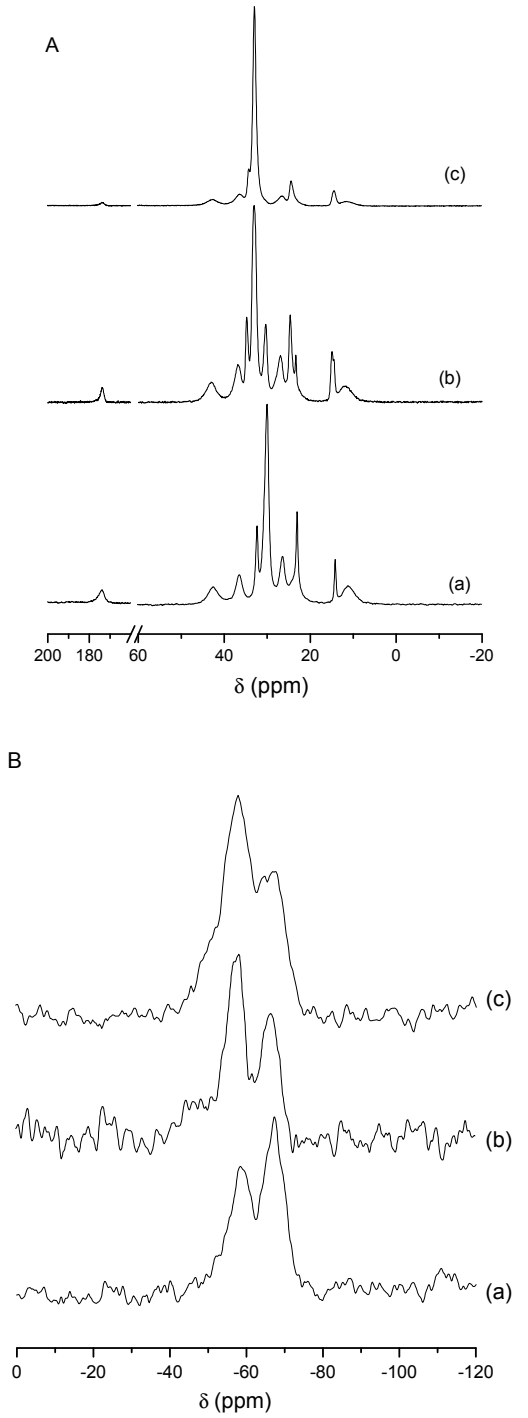

Figure S1. ^{13}C CP/MAS (A) and ^{29}Si MAS (B) NMR spectra of the m-A(8) (a), AC-m-A(8) (1:600) (b) and m-A(14)[1] (c) mono-amidosils

Symmetric and asymmetric stretching CH_2 modes (ν_sCH_2 and ν_aCH_2, respectively).

The FT-IR ν_sCH_2 and ν_aCH_2 bands of *all-trans* conformations of crystalline alkyl chains appear in the 2846-2849 and 2919-2918 cm^{-1} ranges, respectively.[2,3] In the case of *gauche* conformations, the FT-IR ν_sCH_2 and ν_aCH_2 bands undergo a shift to higher wavenumbers and are typically observed at 2856–2858 and 2924–2928 cm^{-1}, respectively[2,3] The frequency, width and height of the FT-IR ν_sCH_2 and ν_aCH_2 bands are sensitive to the *gauche/trans* conformer ratio and to the intermolecular interactions between the alkyl chains.[3]

In the FT-Raman spectrum of crystalline alkyl chains (*all-trans* conformations) the ν_aCH_2 mode appears as a strong band in the 2884-2878 cm^{-1} region and the ν_sCH_2 mode gives rise to bands at 2930 cm^{-1} (weak, w), 2900-2898 cm^{-1} (medium, m) and 2850-2844 cm^{-1} (strong, S). [2c-e,3,4] In the case of disordered alkyl chains (*gauche* conformations), the Raman ν_aCH_2 mode was reported at 2897-2890 cm^{-1} and the ν_sCH_2 bands typically developed at 2920 cm^{-1} (m), 2904 cm^{-1} (m) and 2858-2853 cm^{-1} (S).[2c-e,3,4] The location and intensity of the Raman ν_sCH_2 mode is complicated because of Fermi resonance between the ν_sCH_2 fundamental with the many overtones of the CH_2 bending (δCH_2) vibrations.[2c,2d, 2e,2e,3b] The ν_sCH_2 mode is affected by coupling to the torsional and rotational motions of the chain.[2c,2d, 2e,3b]

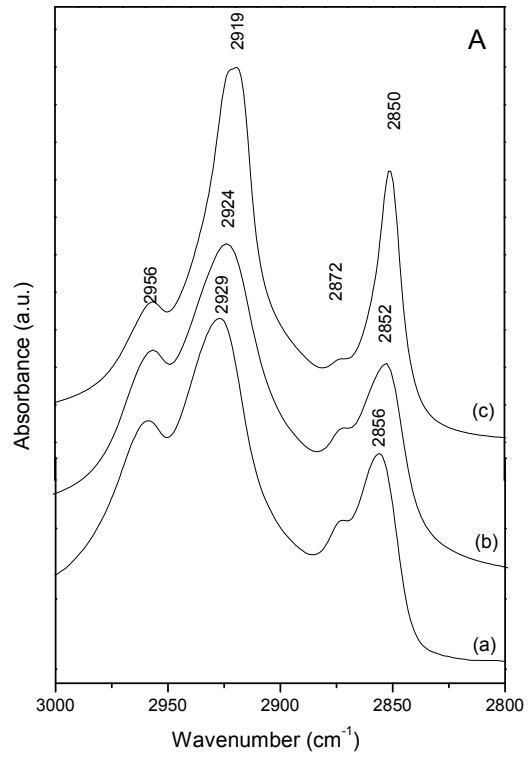

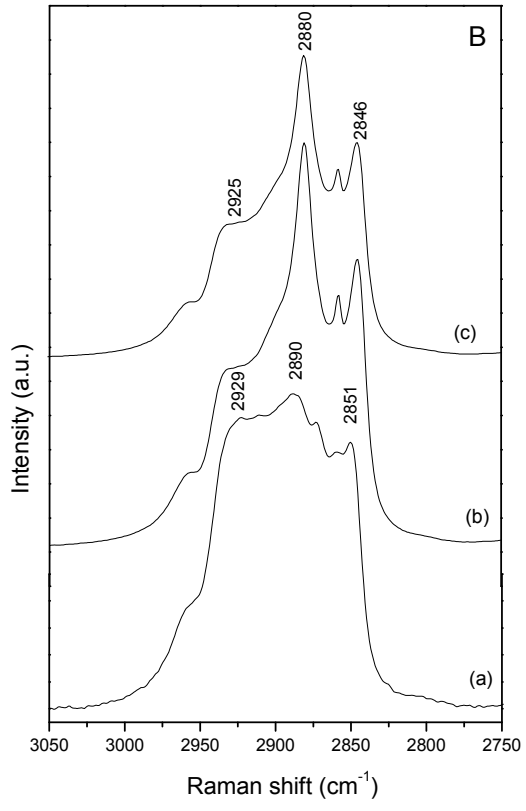

Figure S2. FT-IR (A) and FT-Raman (B) spectra of the m-A(8) (a), AC-m-(8) (1:600) (b) and m-A(14) (c) mono-amidosils in the $\nu_s CH_2$ and $\nu_a CH_2$ regions.

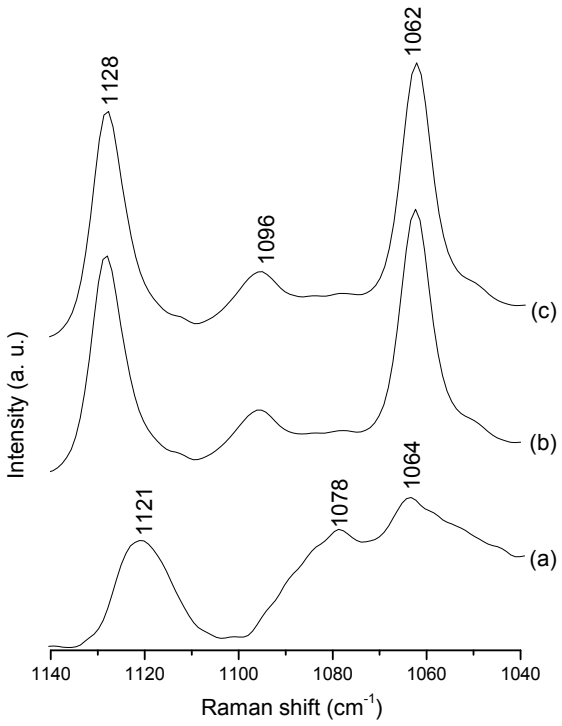

Figure S3. FT-Raman spectra of the m-A(8) (a), AC-m-A(8) (1:600) (b) and m-A(14)[1] (c) mono-amidosils in the νC-C region

"Amide I" and "Amide II" modes

The amide I mode receives a major contribution from the C=O stretching vibration and minor contributions from the C-N stretching and C-C-N deformation vibrations.[5] The amide I mode is sensitive to the specificity and strength of hydrogen bonding.[6] Usually the amide I band envelope consists of several distinct components that correspond to different environments of the C=O group, usually named aggregates. Within this spectral region (1800-1600 cm^{-1}) the lower the wavenumber of the component intensity maximum, the stronger the hydrogen-bonded aggregate is. The amide II mode, mainly associated with the N-H in-plane bending vibration is sensitive to chain conformation and intermolecular hydrogen bonding, providing information about the distribution of hydrogen bond strengths.[6a] In the amide II interval (1600-1500 cm^{-1}) components with higher wavenumber intensity maxima are correlated with stronger hydrogen-bonded aggregates.

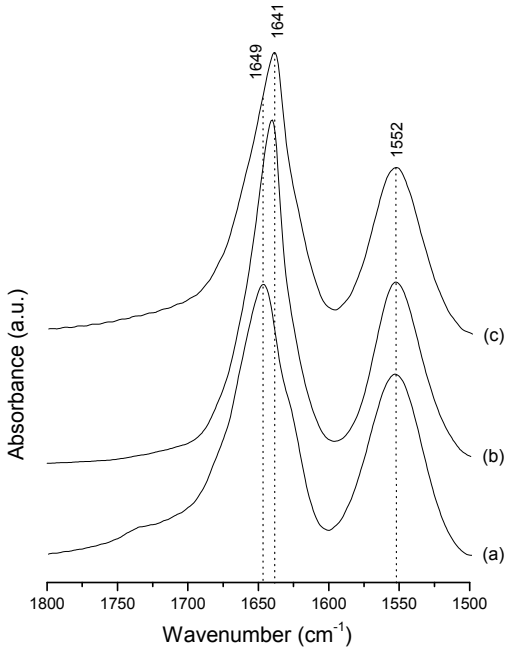

Figure S4. FT-IR spectra of the m-A(8) (a), as-prepared AC-m-(8) (1:600) (b) and m-A(14)[1] (c) mono-amidosils in the amide I and amide II regions.

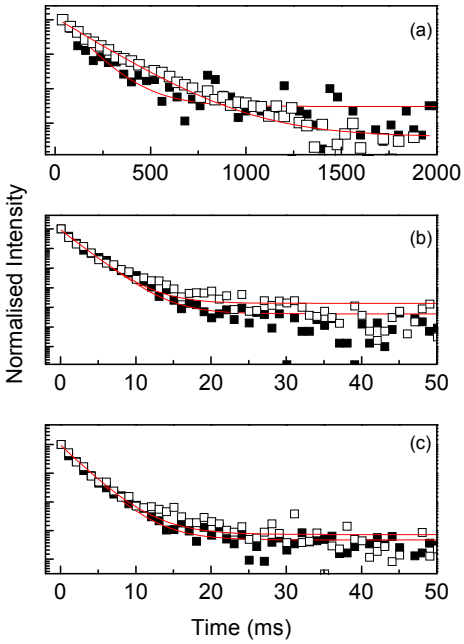

Figure S5. Emission decay curves of m-A(8) (open squares) and AC-m-A(8) (1:600) (solid squares) mono-amidosils excited at 360 nm and monitored at 500 nm (a), 455 nm (b) and 427 nm (c). The solid lines represent the best fit of the data using a single exponential function.

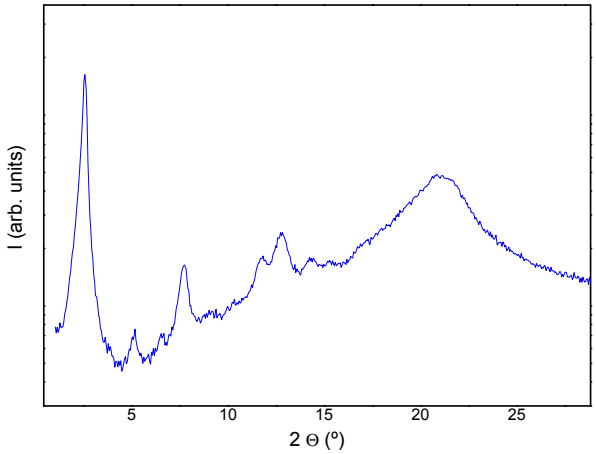

Figure S6. Room temperature XRD pattern of the AC-m-A(8) (1:600) mono-amidosil recorded two months after performing the the two heating cycles described in Figure 4.

Notes and references

[a] *Chemistry Department, University of Trás-os-Montes e Alto Douro, 5001-801 Vila Real, Portugal, Fax: +351 259 350 480; Tel: +351 275 259 350 253; E-mail: vbermude@utad.pt.*
[b] *CQ-VR, University of Trás-os-Montes e Alto Douro, 5001-801 Vila Real, Portugal, Fax: +351 259 350 480; Tel: +351 275 259 350 253; E-mail: vbermude@utad.pt.*
[c] *Chemistry Department, Faculty of Sciences, University of Beira Interior 6200-001 Covilhã, Portugal, Fax: +351 259 329 730; Tel: +351 275 329 174 E-mail: pjsa@ubi.pt*
[d] *Physics Department and CICECO, University of Aveiro, 3810-193 Aveiro, Portugal, Fax: +351-234-424965; Tel: +351-234-370946; E-mail: lcarlos@fis.ua.pt*
[e] *CICS- UBI – Centro de Investigação em Ciências de Saúde, University of Beira Interior, 6200-001 Covilhã, Portugal, Fax: +351 259 329 730; Tel: +351 275 329 174 E-mail: pjsa@ubi.pt*

1 (a) L. D. Carlos, V. de Zea Bermudez, V. S. Amaral, S. C. Nunes, N. J. O. Silva, R. A. Sá Ferreira, C. V. Santilli, D. Ostrovskii, J. Rocha, *Adv. Mater.,* 2007**, 19**, 341; (b) S. C. Nunes, PhD Dissertation, 2007, Vila Real (Portugal), 92678/1/2 SD (http://opac.sde.utad.pt/geral/)
2 (a) M. D. Porter, T. B. Bright, D. L. Allara, C. E. D. Childsey, *J. Am. Chem. Soc.,* 1987**, 109,** 3559; (b) S. Singh, J. Wegmann, K. Albert, K. Muller, *J. Phys. Chem. B,* 2002, **106**, 878; (c) N. V. Venkataram, S. Vasudevan, *J Phys Chem B,* 2001, **105**, 7639; (d) N. V. Venkataram, S. Bhagyalakshmi, S. Vasudevan, R. Seshachi, *Phys. Chem. Chem. Phys.*, 2002, **4**, 4533; (e) R. Wang, G. Baran, S. L. Wunder, *Langmuir,* 2000**, 16**, 6298.
3 (a) R. A. Macphail, H. L. Strauss, R. G. Snyder, C. A. Ellinger, *J. Phys. Chem.,* 1984, **88**, 334; (b) R. G. Snyder, H. L. Strauss, C. A. Ellinger, *J. Phys. Chem.,* 1982**, 86**, 5145.
4 K. G. Brown, E. Bicknell-Brown, M. Ladjadj, *J. Phys. Chem.,* 1987**, 91**, 3436.

(5) T. Miyazawa, T. Shimanouchi, S.-I. Mizushima, *J. Chem. Phys.,* 1956**, 24(2***),* 408.
(6) (a) D. J. Skrovanek, S. E. Howe, P. C. Painter, M. M. Coleman, *Macromolecules,* 1985*,* **18**, 1676; (b) D. J. Skrovanek, P. C. Painter, M. M. Coleman, *Macromolecules,* 1986, **19**, 699; (c) M. M. Coleman, K. H. Lee, D. J. Skrovanek, P. C. Painter, *Macromolecules,* 1986, **19**, 2149.